https://doi.org/10.5194/egusphere-2025-704
Preprint. Discussion started: 6 March 2025

Arctic regional changes revealed by clustering of sea-ice observations

Amélie Simon[12], Pierre Tandeo[13], Florian Sévellec[23], Camille Lique[2]

[1] IMT Atlantique, Lab-STICC, UMR CNRS 6285, 29238, Brest, France
[2] Univ Brest CNRS Ifremer IRD, Laboratoire d'Océanographie Physique et Spatiale (LOPS), Brest, France
[3] ODYSSEY Team-Project, INRIA CNRS, Brest, France

Corresponding author: Amélie Simon (amelie.simon@ifremer.fr)

https://doi.org/10.5194/egusphere-2025-704
Preprint. Discussion started: 6 March 2025

Abstract

Understanding the evolution of Arctic sea-ice is crucial due to its climatic and socio-economic impacts. Usual descriptors (e.g., sea-ice extent, sea-ice age, and ice-free duration) quantify changes but do not account for the full seasonal cycle. Here, using satellite observations of sea-ice concentration over 1979-2023, we perform a k-means clustering of the Arctic sea-ice seasonal cycle, initializing with equal quantile separation and using Mahalanobis distance. We identify four optimal seasonal cycle clusters: open-ocean (no ice year-round), permanent sea-ice (full coverage with a minimum of 70% sea-ice concentration), and two clusters showing ice-free conditions, namely partial and full winter freezing. The latter has larger sea-ice concentration in winter, more abrupt melting and freezing periods, and a shorter ice-free season than the former. The probability of belonging to the open-ocean cluster increased by 1.6% per decade mostly due to cluster spatial expansion on the Eurasian side. The permanent sea-ice decreased by 1.5% per decade with a likelihood reduction in the Canadian side. The partial and full winter freezing clusters do not exhibit any trend but spatial shifts occur. We further diagnose cluster transitions and subsequently infer regions of stabilization and destabilization. The East Siberian and Laptev seas are destabilizing (losing their typical permanent sea-ice seasonal cycle) while the Kara and Chukchi seas have stabilized (experiencing a new typical seasonal cycle, corresponding to the partial winter-freezing cluster). This work provides a new way to describe Arctic regional changes using a statistical framework based on physical behaviours of sea-ice.

Keywords

Arctic sea-ice, seasonal cycle, machine learning, clustering, climate change, satellite dataset, regionalization

https://doi.org/10.5194/egusphere-2025-704
Preprint. Discussion started: 6 March 2025

Introduction

The Arctic region has experienced rapid changes over recent decades that are expected to intensify in the future (Shu et al., 2022). For a global warming of 1°C, the Arctic has warmed by about 2.5 °C. In a 4°C warmer world, the Arctic is projected to be from 7°C to 10°C warmer (IPCC, 2021; their Figure SPM.5). One of the main mechanisms behind this Arctic amplification is the retreat of sea-ice, giving way to an open-ocean that captures more solar radiation, an effect called surface albedo feedback (Pithan and Mauritsen, 2014; Goosse et al., 2018). The observed Arctic sea-ice loss has been attributed to human influence primarily because of greenhouse gas emissions dominated by carbon dioxide and methane (Eyring et al., 2021 in IPCC, their section 3.4.1.1).

The decline of the Arctic sea-ice has profound implications for the regional environment and for almost four million people living beyond the Arctic circle. Reduced ice cover increases light availability, which can enhance phytoplankton blooms (Vancoppenolle et al., 2013). This, in turn, reshapes the food web structure (Ardyna and Arrigo, 2020) and has significant consequences for fisheries, potentially impacting catch levels and spatial distribution (Stock et al., 2017). The formation and melting of sea ice also largely influences nearly all aspects of life for marine mammals in the Arctic. A delay in winter sea-ice formation can trigger marine mammals' unusual mortality events, as it has been the case in 2018 in the Bering Sea (Siddon et al., 2020). Indigenous hunting opportunities that are dependent on the presence of sea-ice have decreased and shifted in time (Huntington et al., 2017). Besides, new ice-free regions could open industrial shipping routes and offshore oil and gas exploration with associated risks of oil spills, marine mammal strikes and noise pollution and lead to tension between nations (Galley et al., 2013; Huntington et al., 2020).

The sea-ice retreat not only affects the Arctic locally but also plays a pivotal role in the global Earth's radiative budget (Forster et al., 2021 in IPCC, their section 7.4.2.3) and a potential role in the modulation of remote large-scale oceanic and

https://doi.org/10.5194/egusphere-2025-704
Preprint. Discussion started: 6 March 2025

atmospheric circulation, known as Arctic teleconnections (Deser et al., 2015; Cohen et al., 2020; Simon et al., 2021; Smith et al., 2022). Therefore, describing the evolution of the Arctic sea ice on a dynamic basis is important due to its fast evolution, which has implications for both local and global climate and socio-economic systems.

Different methods have been classically used in the literature to describe the recent changes in Arctic sea-ice. Most of them are based on the analysis of sea-ice concentration (SIC), which is obtained from satellite measurements since 1979 over the full Arctic region. In comparison, observational datasets of sea-ice thickness are available only for less than two decades and are still associated with large uncertainties (Ricker et al. 2017). The sea-ice area (SIA; integral sum of the product of SIC and area of all grid cells) or the sea-ice extent (SIE; integral sum of the areas of all grid cells with at least 15% ice concentration) enable to highlight years with exceptionally low September sea-ice cover, such as 2012 and to a smaller extent 2007, 2016 and 2020 (Parkinson and Comiso, 2013; Petty et al., 2018; Gulev et al., 2021 in IPCC, their Figure 2.20; Bushuk et al., 2024) or quantify long-term trends. For instance, the September SIE exhibits a decreasing trend of - 12.8 ± 2.3% per decade over the period 1979 to 2018 (SROCC, IPCC, 2019; Meier and Stroeve, 2022). However, trends of SIA or SIE only inform about changes in regime from ice to open-ocean and do not consider changes in sea-ice features.

Two main diagnostics have been proposed to document these changes. First, the age of sea-ice categorizes sea-ice into three types: open-water, first-year ice and multi-year ice (Kwok et al., 2007; Regan et al., 2023). Maslanik et al. (2011) show a strong decrease in the proportion of multiyear ice in the Arctic Ocean during the 1980-2011 period, especially in the Canadian sector. A second diagnostic deals with the duration of the ice-free period, and quantifies the timing of the transition between the freezing and melting seasons. The recent Arctic sea-ice reduction has resulted in a longer ice-free season (~ 5-10 days per decade), due to both earlier ice retreat and later ice advance (Stammerjohn et al., 2012; Stroeve et al., 2014; Lebrun et al., 2019), especially in the Chukchi, East Greenland and northeast Barents seas (Markus et al., 2009; Parkinson, 2014; Johnson & Eicken, 2016). However, these

https://doi.org/10.5194/egusphere-2025-704
Preprint. Discussion started: 6 March 2025

diagnostics do not consider the full seasonal cycle of sea-ice, and thus do not inform on the sea-ice dynamics including melting and growth behaviour.

These three ways of describing the variations in Arctic SIC (trend of SIE, type of sea-ice, ice-free duration), without considering directly the full sea-ice seasonal cycle, have nonetheless highlighted changes in the shape of the sea-ice seasonal cycle: (i) the trend in SIE depends on the season, being maximum in late summer (Fox-Kemper et al., 2021 in IPCC, their Figure 9.13; Meier and Stroeve, 2022), (ii) Arctic sea ice has shifted to younger ice between 1979 and 2018 (IPCC, 2019) and (iii) the trend of later ice advance is expected to eventually double that of earlier retreat over this century, shifting the ice-free season into autumn (Lebrun et al., 2019). Here, in this paper, we describe the evolution of the Arctic by delimiting spatio-temporal regions having a common type of seasonal cycle.

Regionalizations of the Arctic have been proposed previously. Parkinson et al., (1978) divided the Arctic into 8 regions based on either geographical boundaries or physical criteria (e.g.; the Central Arctic encompassing the largest mass of perennial sea-ice or the Greenland Sea which allows for the only deep-water connection within the Arctic Basin). This regionalization was expanded by splitting regions into individual seas to distinguish the behaviour of the Arctic coastal regions, resulting in considering up to 15 or 18 regions (Meier et al., 2007; Peng and Meier, 2018). Besides, five climatic regions of the Arctic have been defined using multiannual averages of a number of meteorological elements computed for the first half of the 20th century: Atlantic, Siberian, Pacific, Canadian and Baffin Bay regions (Przybylak, 2002, 2007). Other regionalizations have been used to assess the influence on lower latitude climates of Arctic sea-ice loss from specific areas (5 to 7 regions; Levine et al., 2021; Delhaye et al., 2024). However, the criteria for the boundaries of these proposed regions are hard to determine and somewhat arbitrary. The originality of our analysis also resides in the fact that we regionalize the Arctic based on physical criteria of the dynamics of the sea-ice seasonal cycle, therefore without imposing pre-defined regions. To do so, we set up a clustering method (unsupervised machine learning).

Dynamical regionalizations determined from clustering methods applied to

https://doi.org/10.5194/egusphere-2025-704
Preprint. Discussion started: 6 March 2025

ocean temperature profiles have been shown to be an efficient tool, to capture coherent physical changes of e.g. the water column during an El Niño event (Houghton and Wilson, 2020) or heat distribution in the North Atlantic (Maze et al., 2017). The same conceptual methodology has also been applied to the polar regions. In the Antarctic, Wachter et al. (2021) described the spatio-temporal sea-ice variability and documented significant spatial shifts during 1979-1998 and 1999-2018 by means of 10 clusters based on the seasonal cycle of sea-ice. In the Arctic, Valko (2014) proposed a regionalization based on geographic and geopolitical indicators, ending up with respectively two and three clusters, and Johannessen et al. (2016) identified 6 major regions by clustering annual average of surface air temperature. The boundaries of the defined clusters coincide with the outlines of the continents and the averaged position of the sea-ice edge. However, no spatio-temporal regionalization based on the clustering of the Arctic seasonal cycle of sea-ice has been proposed so far.

In this paper, we identify for the first time spatio-temporal regions of the Arctic based on the natural variability of the seasonal cycle of Arctic sea-ice. We apply a k-means clustering method to determine regions based on their belonging to a given type of seasonal cycle, the regions having borders evolving in time. In section 2, the dataset, domain of interest and clustering method are detailed. The results of the clustering are displayed in section 3, first analyzing the clustering outputs of the Arctic sea-ice seasonal cycle, then examining the probability for a given region to belong to each cluster, and finally investigating the temporal evolution of the clusters by introducing a new diagnostic labelling the decadal and multidecadal shift of the Arctic sea-ice features. Conclusions and discussion follow in section 4.

2. Data and Clustering Method

2.1 Sea-ice concentration (SIC)

The National Snow and Ice Data Center (NSIDC) provides gridded sea ice concentration (SIC) fields on a 25 km polar stereographic projection obtained from passive microwave satellite measurements on daily temporal resolutions. We use the

https://doi.org/10.5194/egusphere-2025-704
Preprint. Discussion started: 6 March 2025

climate data record (CDR) product (Meier et al., 2021), which is based on the most recent approach combining the NASA team (NT; Cavalieri et al., 1984) and the bootstrap (BT; Comiso et al., 1986) algorithms. Because of the tendency of passive microwave measurements to underestimate concentration, the CDR chooses the higher concentration between the NT and BT algorithms and assigns it to each grid cell. The pole hole - the region around the North Pole where satellite measurements are unavailable - is filled from the average concentration of the circle of surrounding adjacent grid cells. The size of the pole hole has diminished over time due to advancements in satellite technology. We utilize daily data from January 1979 to December 2023, using linear interpolation for the few missing data and compute mean values every 5 days. The 29 February of every bissextile year is removed before computing the 5-day mean. We choose this 5-day temporal resolution as similar results are found for a daily temporal resolution whereas a monthly temporal resolution shows small differences in the spatial distribution of clusters.

2.2 Studied domain

The study considers the ocean above 55°N. The description of the domain is based on the delimitation provided by NSIDC (Meier et al., 2023) and encompasses 15 classically predefined regions (Figure 1). The bathymetric data is derived from the GEBCO 2024 Grid (GEBCO Compilation Group, 2024).

https://doi.org/10.5194/egusphere-2025-704
Preprint. Discussion started: 6 March 2025

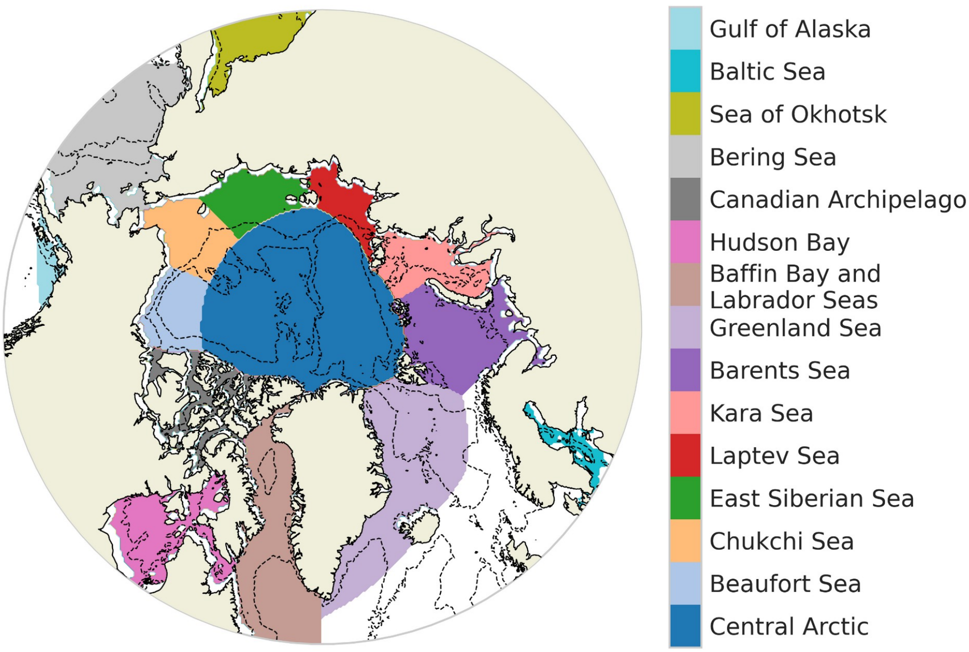

Figure 1: Geographical decomposition of the Arctic Ocean (defined as ocean above 55°N) into 15 regions following Meier et al. (2023). Bathymetry contours -100 m and -2000 m are drawn with a dotted line.

2.3 Clustering set up

We consider all oceanic grid cells above 55°N having a non-zero sea-ice seasonal cycle. Hence, the number of considered grid cells depends on the year. Grid cells with a zero sea-ice seasonal cycle are reintroduced after the clustering in order to define an open-ocean cluster. This enables a clear separation between regimes with and without sea-ice. The input data of our clustering are all the seasonal cycles of every considered grid cell during the considered period. In practice, we are thus working with a matrix with rows containing every considered grid cell of the period 1979-2023, here called points (1123710 elements) and columns containing every time step for one year, here 5-day mean (73 elements).

We implement a k-means clustering algorithm, which is an unsupervised

https://doi.org/10.5194/egusphere-2025-704
Preprint. Discussion started: 6 March 2025

machine learning method that groups data into subsamples sharing common features (Jain et al., 2010). It has the advantage of being non-parametric as our data distribution is strongly non-Gaussian. Indeed, SIC is bounded between 0 and 1 with high occurrences of values close to 0 and 1. It is an iterative method that minimizes a cost function being the sum of the squared distance between each seasonal cycle and its nearest cluster center (also called centroid). The initialization of centroids using k-means++ concept (the first centroid is chosen randomly, the second is the farthest-away, the third the farthest-away of the first and second, and so on) has been tested and is partly influencing our results. Therefore, we choose a different initialization strategy. We initialize the centroids based on seasonal cycles of equal quantile separation. The quantiles are calculated over all the seasonal cycles considered in this study. For a clustering involving two clusters, the initializations are the two seasonal cycles of 33% and 66% quantiles of all seasonal cycles; for a clustering involving three clusters, the initializations are the three seasonal cycles of 0.25, 0.5, and 0.75 quantiles, and so on. This favours initial centroids far from each other to avoid iterating over a local minimum and the clustering is thus deterministic (i.e., it does not present any random aspect).

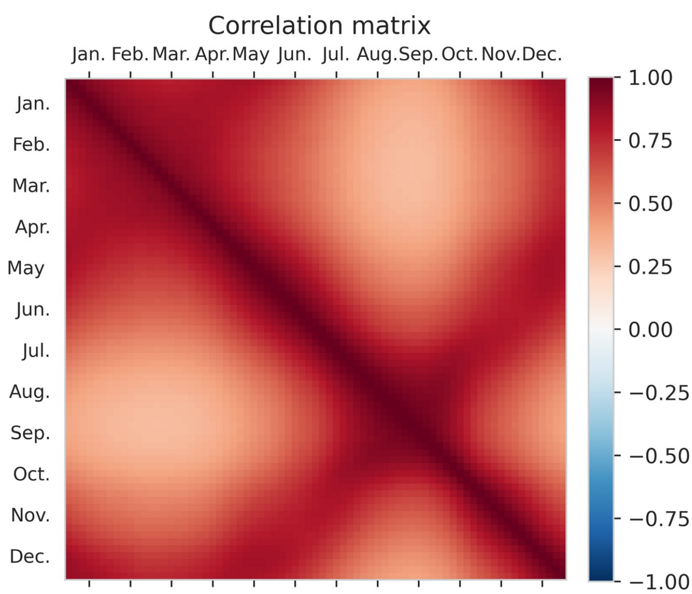

Figure 2: Correlation matrix of the 5-day mean sea-ice concentration above 55°N

https://doi.org/10.5194/egusphere-2025-704
Preprint. Discussion started: 6 March 2025

The clustering algorithm is based on the calculation of distances. The Euclidean distance is often used in similar methods, yet, here, we choose to use the Mahalanobis distance to constrain the clustering with physical information. All the combinations of 5-day mean SIC have a positive correlation (as shown in Figure 2 by the correlation matrix for the period 1979-2023. Notably, a strong correlation exists between spring and autumn (June and November), while the weakest correlations are between summer and winter (March and September, minimum correlation is 0.31). As data are correlated, a privileged direction exists when plotting the SIC for all grid cells and all years of a given date (5-day mean) against another date. We consider this physical relation by using the Mahalanobis distance (which we defined as an Euclidean scalar product normalized by the inverse of the correlation matrix) in the clustering algorithm. A 5-day mean SIC strongly correlated with another (such as spring and autumn) has a reduced distance compared with Euclidean distance. Therefore, using the Mahalanobis distance helps the clustering algorithm to follow the direction of the correlation and capture the elongated shapes of clusters.

We note that, as we want to conserve the physical information of the variability intensity for each 5-day mean SIC, we do not normalize the distance by the covariance matrix (as usually done for the Mahalanobis distance) but by the correlation matrix that only takes into account relation between different 5-day mean SIC. As a result, a 5-day mean SIC with weak variability (as in winter) will have a smaller impact on the total seasonal cycle than a 5-day with larger variability (as in summer). Therefore, we do not modify the relative weight (based on the variability) of each 5-day mean SIC.

The number of clusters needs to be specified for the k-means clustering. We define the optimal number of clusters based on the Silhouette coefficient (Rousseeuw, 1987; Houghton and Wilson, 2020) that measures the quality of the clustering when seeking for compact and well-separated clusters. We rely on the Silhouette_sample function from the python package sklearn.metrics (Pedregosa et al., 2011), which calculates the Silhouette coefficient for every point as $(b - a) / \max(a, b)$ where a is the mean intra-cluster distance and b is the mean nearest-cluster

https://doi.org/10.5194/egusphere-2025-704
Preprint. Discussion started: 6 March 2025

distance for each point. Each point is labelled as being in a cluster using the k-means clustering (with correlation-based Mahalanobis distance), while the distance used in the calculation of *a* and *b* is the Euclidean distance. The larger the Silhouette coefficient is (bounded between -1 to 1), the farthest the centroids are from each other and the more grouped are the points of the same cluster. We have computed the clustering and its associated Silhouette for a number of clusters ranging from 2 to 20 (Figure 3). As the distribution of the Silhouette coefficient is asymmetric, we sort this sensitivity test using the median. The maximum median Silhouette coefficient gives an optimal number of clusters, which is 3 in our case (Figure 3). Therefore, after reintroducing the open-ocean grid cell for each year, we end up with four clusters (three optimal clusters obtained using the Silhouette coefficient for non-zero seasonal cycle of sea-ice and the open-ocean cluster reintroduced manually).

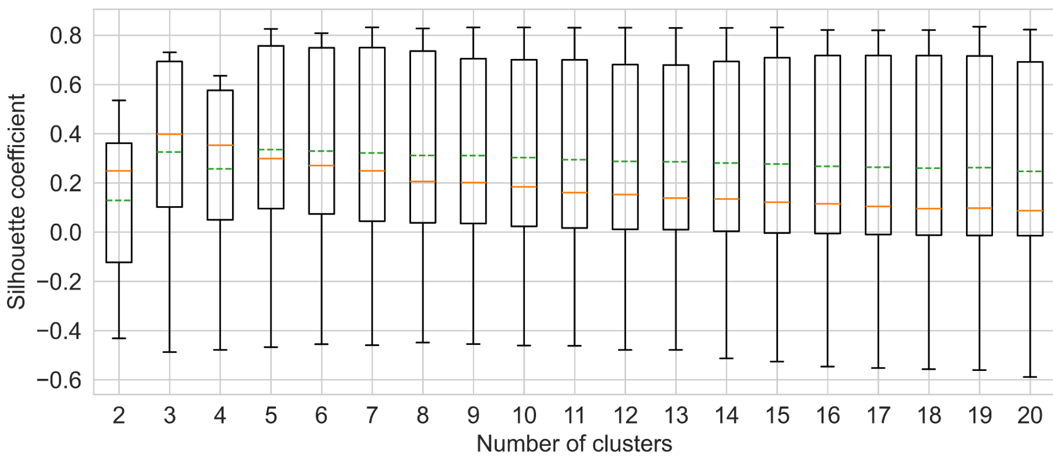

Figure 3: Boxplot of the Silhouette coefficient for a number of clusters from 2 to 20. The box extends from the first quartile (25%) to the third quartile (75%) of the Silhouette coefficient. The whiskers indicate the 1st and 99th percentiles. The green-dashed and orange-solid lines indicate the mean and median values (50%), respectively.

https://doi.org/10.5194/egusphere-2025-704
Preprint. Discussion started: 6 March 2025

3. Results

3.1 Clustering outputs

One of the two outputs of the clustering method is the centroids (optimal cluster centers), which correspond to the four types of seasonal cycles (Figure 4a). They exhibit the expected physical behavior that, due to the thermal inertia of the ice and indirect processes involving the ocean and atmosphere, the maximum sea-ice coverage (in March) follows the minimum solar insolation by around 3 months, and the minimum sea-ice coverage (in September) occurs around 3 months after the maximum solar insolation (Parkinson et al. 1987).

The four types of seasonal cycles present different features. The 'open-ocean' cluster has a SIC equal to zero all year round, which was sought for our analysis and represents year-long ice-free conditions. The second cluster, referred to as 'partial winter-freezing', has a quasi-sinusoidal shape with a mean SIC ranging from ~70% in March to no-ice in summer (early August to mid-October). The 'full winter-freezing' cluster is bound to a SIC of 100% from mid-November to April and to almost no-ice by mid-September. For this cluster, the sea-ice completely melts in 5 months (from April to September) and totally freezes up in 2 months (from mid-September to mid-November). The full winter-freezing cluster has more abrupt seasonal changes compared to the partial winter-freezing cluster. The permanent sea-ice cluster corresponds to regions that are sea ice covered all year round, with only a partial melting between May and October, peaking at its minimum in late August (mean SIC around 70%). The three clusters with sea-ice have different starting dates of melting (May for the permanent sea-ice cluster, April for the full winter-freezing one and March for the partial winter-freezing one) and for freeze up (late-August for the permanent sea-ice cluster, October for the full winter-freezing cluster and mid-October for the partial winter-freezing cluster). The resulting ice-free period duration is thus around 2 months for the full winter-freezing cluster and 3 months for the partial winter-freezing cluster.

https://doi.org/10.5194/egusphere-2025-704
Preprint. Discussion started: 6 March 2025

This clustering analysis shed light on sea-ice precursors. In our optimal data separation analysis, it appears that when considering areas totally covered by ice in winter, the starting date of melting is a good predictor for ice-free conditions in summer. Considering a given location fully ice-covered in a given winter, our clustering results suggest that when the sea ice starts to melt in April, the seasonal cycle will follow the full winter-freezing cluster and be ice-free the next summer. In contrast, when the melting starts one month later (in May) the seasonal cycle will follow the permanent sea-ice cluster and the considered location will not be ice-free in summer. Besides, the freezing date for areas free of ice could differentiate between the partial winter-freezing and full winter freezing clusters and subsequently predict full ice conditions in the following winter. In our clustering, a freezing starting in October totally freezes in winter which is not the case if the freezing starts in November, having a maximum of about 70% SIC in March. Therefore, it appears that, for ice-free conditions in summer, the starting date of freezing is a good predictor for the apparition of full ice conditions in the next winter.

https://doi.org/10.5194/egusphere-2025-704
Preprint. Discussion started: 6 March 2025

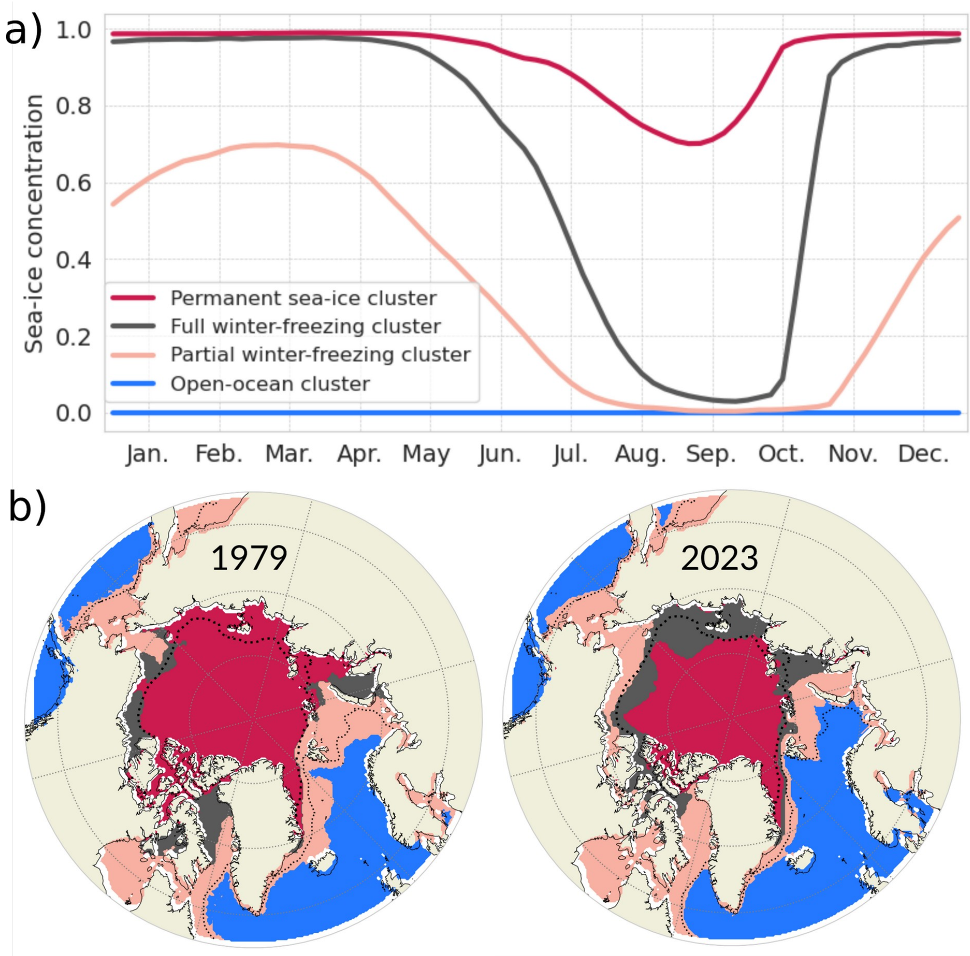

Figure 4: (a) Four types of seasonal cycles determined by the clustering and (b) their corresponding regions for the years 1979 (left) and 2023 (right). The dotted thin and thick lines are the mean SIC of 0.15 and 0.8 for the period 1979-2023, respectively.

The second output of the clustering method is the connection of each grid point to a given cluster. The clustering method associates the sea-ice seasonal cycle of each year and each grid cell to the nearest seasonal cycle type (based on the smallest Mahalanobis distance between the seasonal cycle of the point and the seasonal cycle of the centroids). Without giving any information to the clustering algorithm on the spatial and temporal dependency between the seasonal cycles, we

https://doi.org/10.5194/egusphere-2025-704
Preprint. Discussion started: 6 March 2025

retrieve spatially consistent and continuous patterns (Figure 4b). The clusters are sorted going toward the pole as follows: the open-ocean cluster, the partial winter-freezing cluster, the full winter-freezing cluster and the permanent sea-ice cluster. The first three clusters exhibit wavy bands surrounding the pole, and the permanent sea-ice cluster sits over the pole. More details on the description of the regions will follow based on our probabilistic framework (section 3.2.2).

3.2 Probability to belong to a cluster

3.2.1 Calculation

As a given seasonal cycle can be in between two or more seasonal cycle centroids, we calculate the probability P of a grid point to belong to each cluster. We define the vectors ***x*** and ***c(k)***, corresponding respectively to the SIC observed at a grid cell over a year (i.e., 73 intervals of 5 days) and the cluster centroid k. These are of dimension (73x1) and are written as:

$$\mathbf{x} = [x_1, \ldots, x_{73}]^T; \quad \mathbf{c(k)} = [c_1(k), \ldots, c_{73}(k)]^T \qquad (1)$$

The Mahalanobis distance scalar between the point x and the centroids k is defined as follows:

$$d_{x,c(k)} = \sqrt{(\mathbf{x} - \mathbf{c(k)})^T \mathbf{M_{cor}}^{-1} (\mathbf{x} - \mathbf{c(k)})} \qquad (2)$$

with $\mathbf{M_{cor}}$, the correlation matrix of dimension (73x73)

The probability P reads:

$$P(x,k) = \left[\sum_{l=1}^{n_c} \left(\frac{d_{x,c(k)}}{d_{x,c(l)}} \right)^2 \right]^{-1} \qquad (3)$$

with $n_c$the total number of clusters (4 in our case). *P* ranges from 0 to 1 and the sum over the fours clusters of *P* equals 1. In other words, the probability of being in a cluster is set by the distance of one seasonal cycle to a seasonal cycle centroid,

https://doi.org/10.5194/egusphere-2025-704
Preprint. Discussion started: 6 March 2025

normalized by the sum of the distance to all clusters. This means that we use a "fuzzy" k-means clustering where the assignment is soft (each data point can be a member of multiple clusters) in contrast to a hard or crisp assignment (each data point is assigned to a single cluster; Jain et al., 2010).

We call the total probability, Pt, the normalized area weighted probability over all grid cells. We sum, for each year, the probability weighted by the area of each grid cell over all grid cells divided by the sum of the probability weighted by the area of each grid cell over all clusters and all grid cells. Pt can be written as:

$$Pt(k) = \frac{\sum_x P(x,k)\cdot\mathrm{area}(x)}{\sum_k \sum_x P(x,k)\cdot\mathrm{area}(x)} \qquad (4)$$

3.2.2 Map of probability

After attributing each point to a probability of belonging to each cluster per year (using equation (3)), we average this probability over three periods of 15 years (Figure 5). During the first period (1979-1993), the Nordic Seas, the Bering Sea and the Gulf of Alaska belonged solely to the open-ocean cluster (free of ice). The central Arctic belongs to the permanent sea-ice cluster. The edge of the 0.3 probability of belonging to the permanent sea-ice clusters of the period 1979-1993 follows the border of the Marginal Ice Zone (0.8 SIC) located in the Central Arctic. The belt shape between the Central Arctic and the open-ocean belongs to more than one cluster. In the first order, these regions have an almost equal probability of belonging to one of the four clusters.

In the subsequent periods (1994-2008 and 2009-2023), the open-ocean cluster continuously expanded in the Barents Sea, East Greenland Sea and Labrador Sea. In these same regions, the other three clusters (partial winter-freezing, full winter-freezing and permanent sea ice clusters) retract. No major cluster changes are seen in the Bering Sea, Kara Sea, southern Hudson Bay and Canadian Archipelago. The permanent sea-ice cluster exhibits substantial change, with intense shrinking from the Pacific side of the central Arctic, losing areas in a belt shape from the

https://doi.org/10.5194/egusphere-2025-704
Preprint. Discussion started: 6 March 2025

Beaufort Sea to the Laptev Sea. This indicates increasingly frequent summer ice-free conditions during the 1979-2023 period.

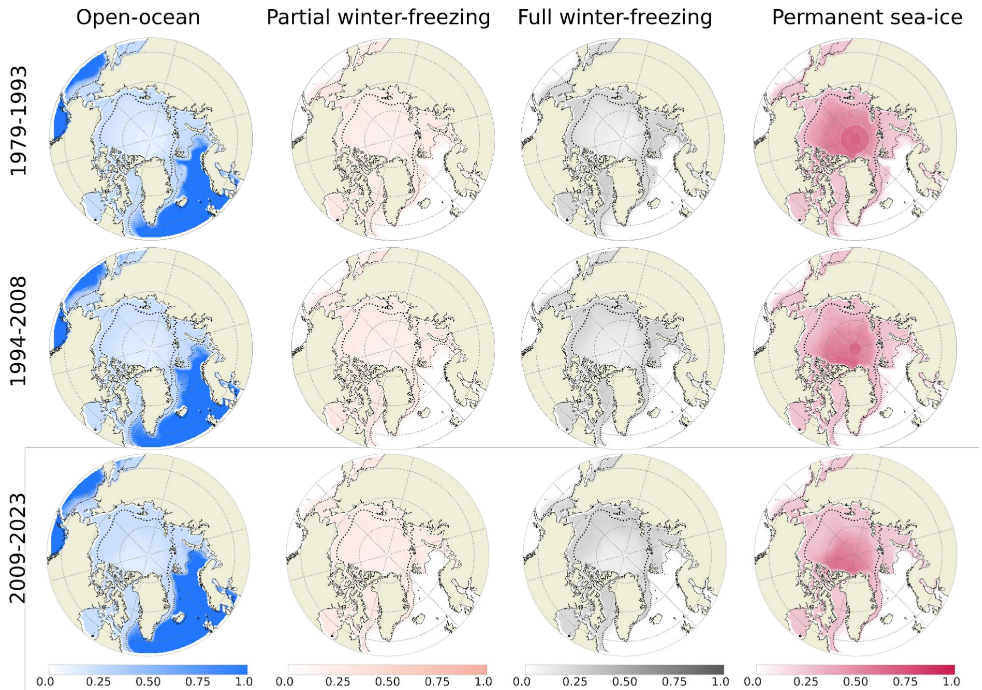

Figure 5: Map of the probability of each cluster: open-ocean (first column), partial winter-freezing (second column), full winter-freezing (third column) and permanent sea-ice (fourth column). Rows correspond to three periods of 15 years: 1979-1993 (top row), 1994-2008 (middle row) and 2009-2023 (bottom row). The dotted thin and thick lines are the mean SIC of 0.15 and 0.8 for the period 1979-2023, respectively. The circle sitting over the north pole is the pole hole (see section 2.1).

Therefore, over the whole period (1979-2023) the open-ocean cluster resides predominantly in the southern part of the Arctic and the permanent sea-ice cluster in the central Arctic. These two clusters have no or weak seasonal changes (constant zero for open-ocean cluster and variation between 100% and 70% SIC for permanent sea-ice). To better shape our understanding of seasonal cycles which strongly change (from no ice to 70% SIC for the partial winter freezing clusters and to 100% SIC for the full winter freezing cluster), we distinguish which areas are mainly associated with

https://doi.org/10.5194/egusphere-2025-704
Preprint. Discussion started: 6 March 2025

each of these two clusters by plotting the difference of probability between these two clusters for the whole period (Figure 6). It displays spatially consistent regions, albeit with weak probability differences (less than 10%). From north to south, between these two clusters, the Central Arctic is dominated by the partial winter-freezing cluster, and then a belt connecting the Baffin Bay to the Kara Sea (except the Chukchi Sea) is dominated by the full winter-freezing cluster. This inner belt, dominated by the full winter freezing cluster, is attached to the coastal Arctic. Further south, this cluster is surrounded by an outer belt from Barents to Hudson Bay and by the Chukchi Sea dominated by the partial winter-freezing cluster. This outer belt corresponds to the edge of the open-ocean cluster.

Thus, the full winter freezing cluster is slightly more likely to occur in coastal areas than the partial winter freezing cluster. This spatial repartition might be explained by the difference in year-round shapes of the seasonal cycles: quasi-sinusoidal for partial winter freezing and asymmetric for full winter freezing. Indeed, Eisenman (2010) demonstrates that the coastlines, by blocking the sea-ice growth, drive the asymmetric seasonal cycle's shape while sea-ice free to grow and melt (not being blocked by land) has a sinusoidal shape. Our results corroborate this finding, albeit in the second order. In the first order, the quasi-sinusoidal and asymmetric shapes of the respective clusters (partial and full winter freezing) share the same areas.

https://doi.org/10.5194/egusphere-2025-704
Preprint. Discussion started: 6 March 2025

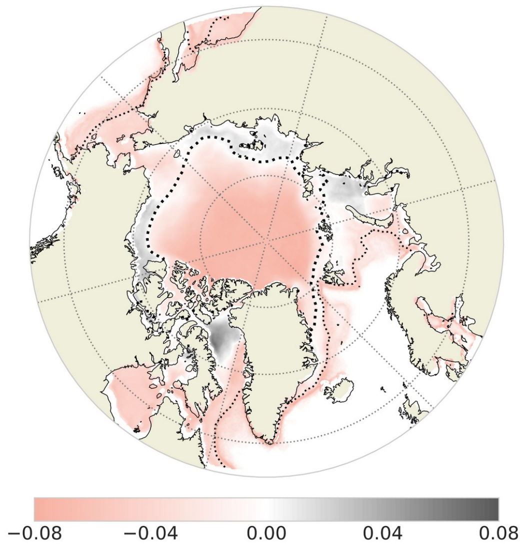

Figure 6: Map of the probability of the full winter-freezing cluster minus the partial winter-freezing cluster averaged over the period 1979-2023. The dotted thin and thick lines are the mean SIC of 0.15 and 0.8 for the period 1979-2023, respectively.

3.3 Time evolution of the clusters

3.3.1 Trend of the probability to belong to a cluster

We analyze the evolution of the total probability to belong to a cluster (normalized area-weighted probability), calculated using equation (4). The probability of belonging to the open-ocean cluster is around 45%, to the permanent sea-ice cluster is around 25% and to the partial winter-freezing cluster is around 17 % and to the full winter-freezing cluster is around 14%. Note that the absolute value reflects our choice of domain, here above 55 °N.

https://doi.org/10.5194/egusphere-2025-704
Preprint. Discussion started: 6 March 2025

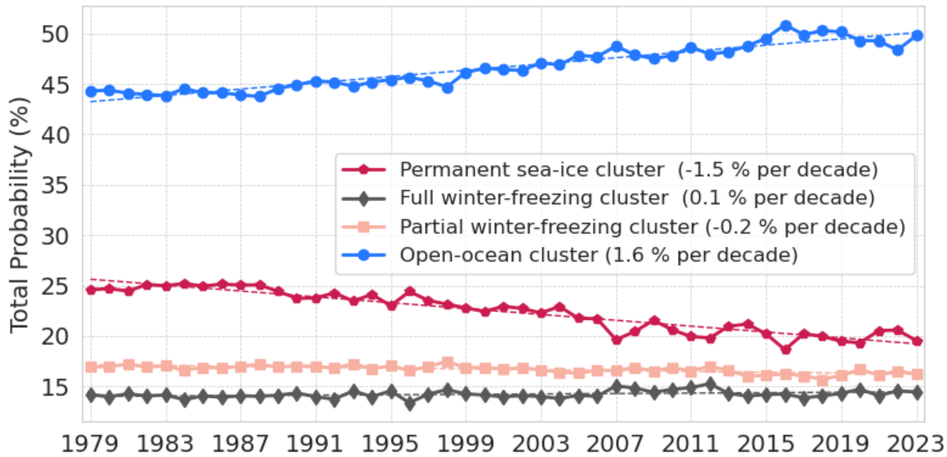

Figure 7: Evolution of the total probability (see Equation (4)) to belong to each cluster.

However, the time evolution of these clusters is in direct relation to the dynamics of the Arctic sea-ice. The probability to belong to the partial and full winter-freezing clusters remains nearly constant. This apparent stationary behavior hides some spatial variations (Figure 5). A linear regression analysis indicates that the trends for the other two clusters are statistically significant, with a p-value less than 0.05 using a Wald Test with a t-distribution. The probability of belonging to the permanent sea-ice cluster overall declines by around 1.5% per decade with an acceleration around the 1997-2012 period. The probability for the open-ocean cluster shows a strong linear trend of about 1.6% per decade, showing a shift in dynamics from seasonal ice to year-round ice-free, especially in the Barents Sea, Greenland Sea and the Labrador Sea. Therefore, most of the probability loss over the last 45 years from the permanent sea-ice cluster is compensated by a gain of the open-ocean cluster, and to a smaller extent, of the full winter-freezing cluster.

https://doi.org/10.5194/egusphere-2025-704
Preprint. Discussion started: 6 March 2025

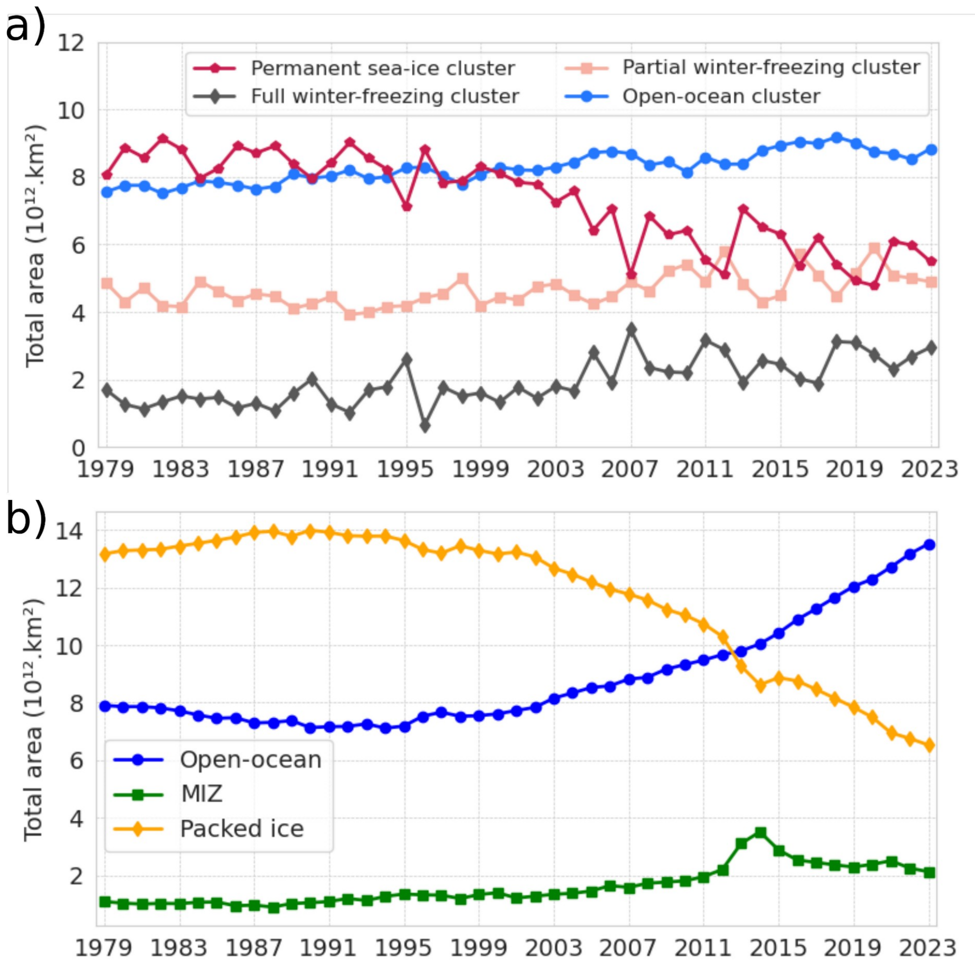

Figure 8: (a) Time series of the total area covered by each of the four clusters. (b) Times series of the area covered by three categories: packed ice, the Marginal Ice Zone (MIZ) and the open-ocean

To investigate the changes in coverage of each cluster, we define the total area of a cluster being the sum over each grid cell having as maximum probability the cluster. We compared the evolution of the total area corresponding to each of our 4 clusters (Figure 8a) with the times series of the decomposition corresponding to a more classical method (Figure 8b), in which the sea ice cover is separated into the packed ice category (0.8 < SIC < 1), the Marginal Ice Zone (MIZ; 0.15 < SIC < 0.8) and the remaining, open-ocean category (SIC< 0.15; Aksenov et al. 2017). The thresholds

https://doi.org/10.5194/egusphere-2025-704
Preprint. Discussion started: 6 March 2025

of 0.15 and 0.8 to define the MIZ are convenient to represent a category with loose and packed ice but somehow arbitrary and other definitions of the MIZ have been proposed in the literature based on dynamical considerations (e.g. Sutherland and Dumont 2018).

Both classification methods highlight distinct aspects of Arctic sea ice dynamics. The traditional classification method captures key trends, particularly the loss of pack ice, which has been decreasing sharply, especially after the early 2000s. Notably, the increasing trend in open ocean areas is pronounced starting around the 2000s when considering SIC below 15%. As also shown in several studies (e.g. Cocetta et al., 2024) The area of the MIZ has expanded, peaking around 2014, suggesting a transition of formerly packed ice into a more fragmented, seasonal state. Our clustering approach includes an explicit open-ocean cluster to track ice-free regions, revealing a steady increase in its extent, particularly after 2000. Similarly, the permanent sea-ice cluster shows a marked decline, while the partial and full winter-freezing clusters remain relatively stable. This classification provides a more nuanced perspective on the shifting nature of Arctic sea ice.

Looking at the years with marked extremes in September sea ice extent (2007, 2012, 2016 and 2020; see introduction), we see the sea-ice loss signature only in the permanent sea-ice cluster (suggesting a loss of year-round ice cover). Therefore, when considering the full seasonal cycle, these years were exceptional only for the permanent sea-ice cluster.

https://doi.org/10.5194/egusphere-2025-704
Preprint. Discussion started: 6 March 2025

3.4.2 Regime stability and transition

In order to describe the grid-cell evolution of the Arctic sea-ice over the period 1979-2023, we further classify each grid cell into four labels: stable, unstable, destabilization, and stabilization. First, we define a stable regime as a sequence when the cluster having the maximum probability stays the same for at least 10 years in a row, allowing for a tolerance of one year to belong to a different cluster within that period. If this condition is not fulfilled, this is an unstable regime. Sensitivity tests have been performed on this definition, and the results do not change when we apply small definition changes (i.e., 9 to 11 years minimum length of the same cluster with zero to 2 years of tolerance). Second, we label each grid cell as follows:

1. Grid cells being in a unique stable regime over the whole period (1979-2023) are labelled stable;
2. Grid cells belonging to a stable regime until the end of the period and being in an unstable regime before are labelled stabilization;
3. Grid cells being in a stable regime before being in an unstable regime until the end of the period are labelled destabilization;
4. Grid cells being in either an unstable regime during the whole period or one or several stable regimes between periods of unstable regimes are labelled unstable.

https://doi.org/10.5194/egusphere-2025-704
Preprint. Discussion started: 6 March 2025

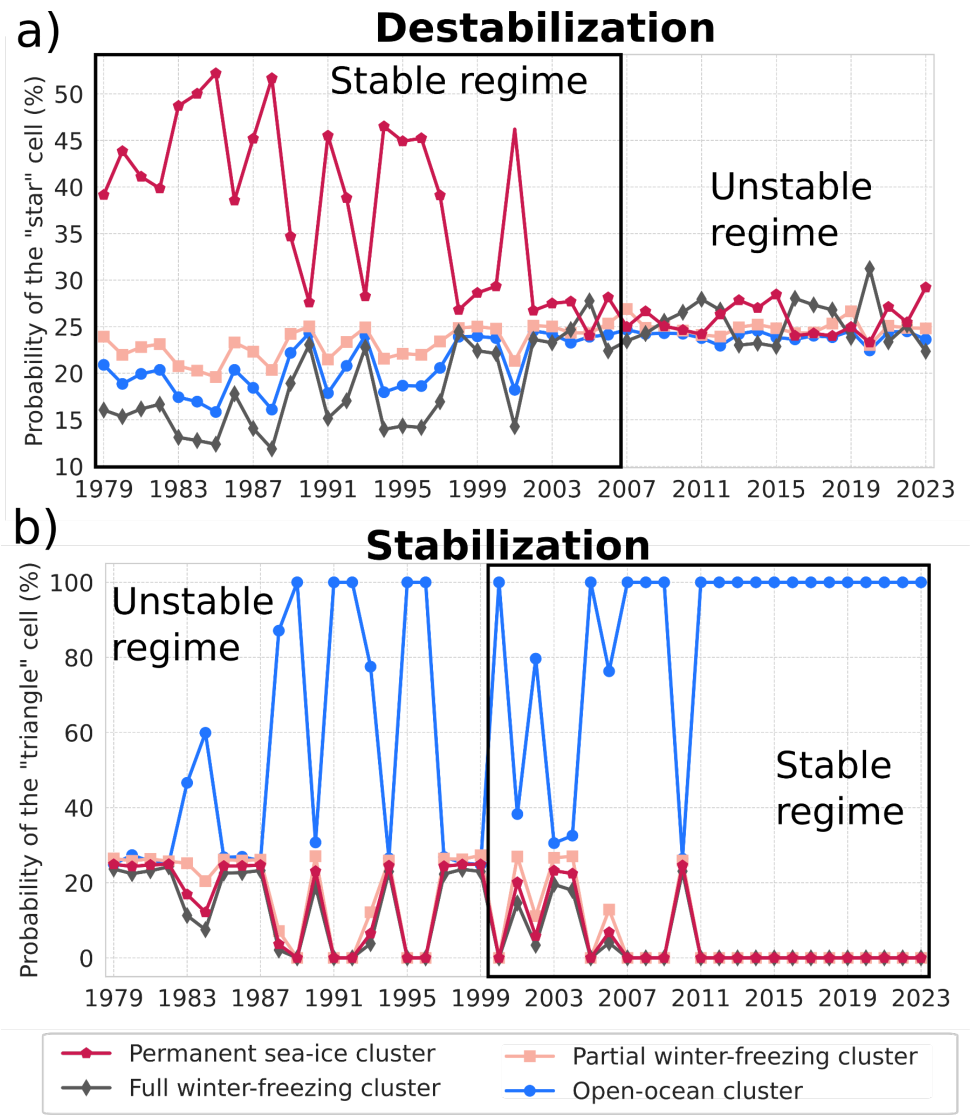

Figure 9: Evolution of clusters at the location denoted by the star (a) and the triangle (b) in Figure 10. The stable regime is delimited by a black rectangle. These locations have been chosen to illustrate the destabilization and stabilization label of the Arctic sea-ice evolution, respectively.

https://doi.org/10.5194/egusphere-2025-704
Preprint. Discussion started: 6 March 2025

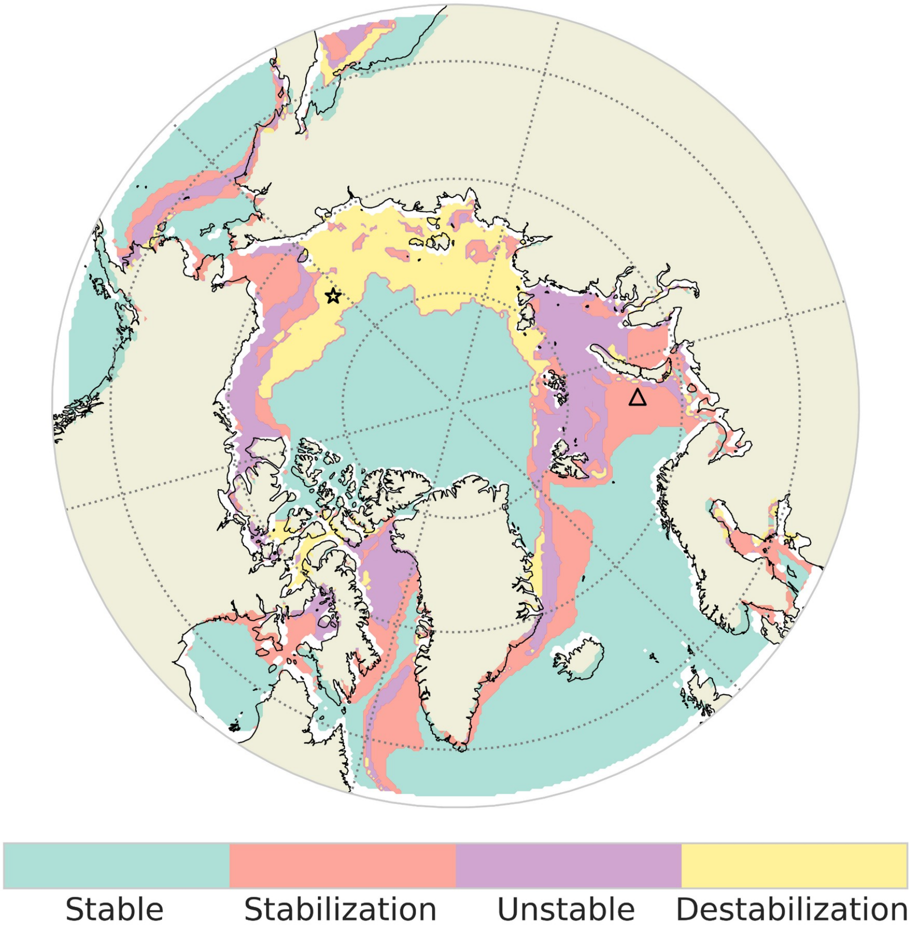

Figure 10: Map of the four labels (stable, stabilization, unstable, and destabilization) used to describe the evolution of Arctic clusters based on sea-ice seasonal cycles. The star and triangle markers indicated the two localizations used to illustrate the destabilization and stabilization in Figure 9, respectively.

As shown Figure 10, the stable region predominantly covers the central part of the Arctic Ocean, including the area around the North Pole, and extends towards the northern parts of the Canadian Archipelago, following most of the regions covered by permanent sea-ice cluster, as well as the ocean regions in the open-ocean cluster. The Hudson Bay and part of the Bering Sea are also labelled stable, although these

https://doi.org/10.5194/egusphere-2025-704
Preprint. Discussion started: 6 March 2025

regions have almost equal probability to belong to the four clusters (from 0.27 to 0.23 depending on the cluster) but the highest probability remains the partial winter-freezing clusters for the whole period in these two regions. The northern Chukchi and Laptev seas correspond to the destabilization region, where there was previously a stable regime of permanent sea-ice cluster and no settled dominant cluster at the end of the period. Therefore, the previously permanent sea-ice cluster has not been replaced by a single cluster but a mix of clusters. The unstable region corresponds to the northern Barents-Kara Seas, Baffin Bay, elongated areas in the eastern East Siberian Sea, the Beaufort, the Chukchi Seas, and the Bering Sea. The stabilization region forms a band from the southern parts of the Kara Sea to the Labrador Sea. It is also present in parts of Hudson Bay, the Chukchi Sea and the Bering Sea.

To quantify the year of transition, we introduce ‘the first year of stabilization’ as the first year when the stable regime occurs until the end of the whole period (Fig. 11a), and ‘the year of destabilization’ as the last year of the stable regime (Fig. 11b). To track cluster shifts, we plot the dominant cluster occurring in the stable regime for the stabilization (Fig. 11c) and the destabilization (Fig. 11d). Stabilization first occurs in the 1979-1990s along the 0.15 SIC contour from the Barents Sea to the Baffin Bay toward open-ocean clusters. During the same early period, the Chukchi Sea and northern Hudson Bay, and around the 2000s the Kara Seas stabilizes toward the partial winter-freezing cluster. Very sparse regions in the central Arctic along the 0.8 SIC contour show a stabilization toward permanent sea-ice at the beginning of the period. On the Pacific side, a later year of stabilization (around 2015) occured in the Bering Sea toward the open-ocean cluster. In the destabilization region (northern Chukchi to the Laptev Seas), the first year of destabilization shows a smooth increasing value when moving northward (Fig. 11b).

The dominant cluster (the cluster having the maximum probability) during the stable regime is displayed Figure 11c and 11d. The destabilization always comes from the loss of permanent sea-ice and stabilization comes mostly from the arrival of the open ocean or partial winter freezing but rarely from the permanent sea-ice cluster.

https://doi.org/10.5194/egusphere-2025-704
Preprint. Discussion started: 6 March 2025

In summary, the four labels illustrate how different regions of the Arctic have experienced changes in stability. The zone from the northern Chukchi to the Laptev Seas has already lost their typical seasonal cycle (destabilization) with the loss of permanent sea-ice and the Barents-Kara Seas and Chukchi Sea have now a new typical seasonal cycle (stabilization) associated with the extension of the open-ocean.

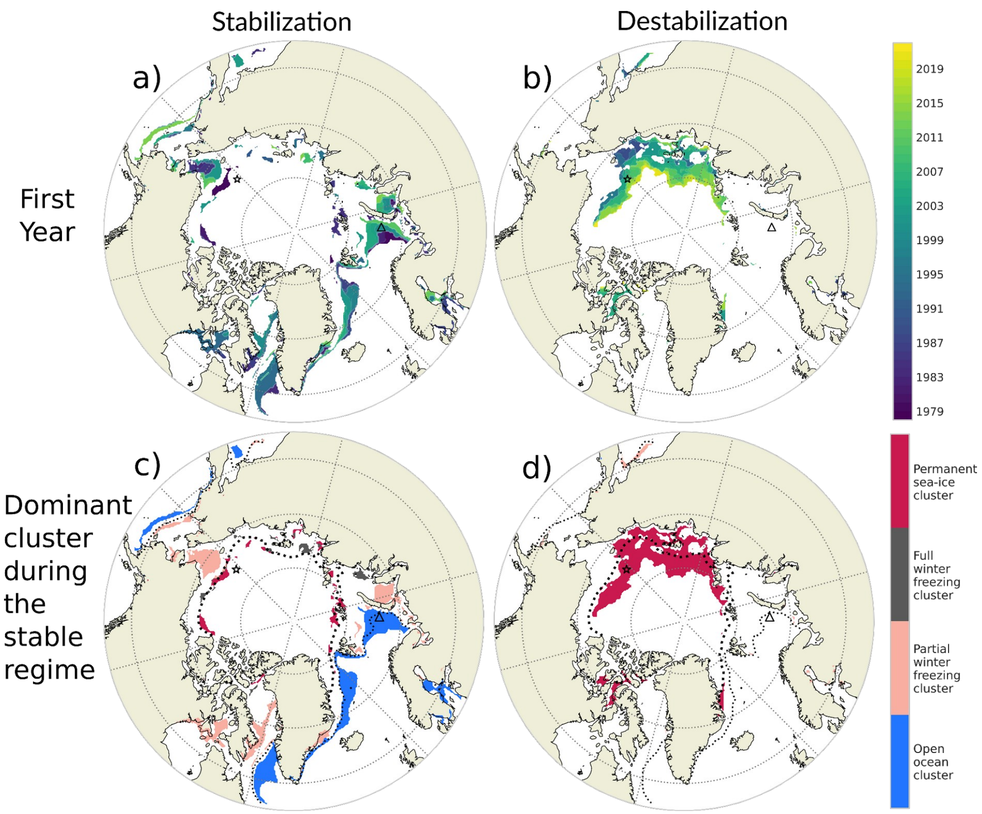

Figure 11: First year of stabilization (a) and destabilization (b) and associated dominant cluster for the stable regime of the stabilization (c) and destabilization (d). The star and triangle markers indicated the two localizations used to illustrate the destabilization and stabilization in Figure 9, respectively.

https://doi.org/10.5194/egusphere-2025-704
Preprint. Discussion started: 6 March 2025

4. Conclusion and Discussion

This paper explores the use of data science methods to study the spatiotemporal evolution of sea-ice in the Arctic over the period 1979-2023. The methodology is based on the clustering (machine learning method) of the full sea-ice seasonal cycle, instead of classic usual descriptors used in previous studies (e.g., sea-ice extent, sea-ice age and ice-free duration). It shows that the Arctic sea-ice changes are optimally described by four clusters of seasonal cycles: the open-ocean cluster (with no ice during the whole year), the permanent sea-ice cluster (total sea-ice coverage with a minimum of 70% sea-ice concentration in September), and two clusters showing ice-free conditions in late summer, namely the partial winter-freezing cluster and the full winter-freezing cluster. The full winter-freezing cluster has a larger sea-ice concentration in winter, displays a more abrupt summer melting and winter freezing and has a shorter ice-free season than the partial winter-freezing one. The central Arctic belongs to the permanent sea-ice cluster. Over the 1979-2023 period, the probability to belong to the open-ocean cluster has increased by 1.6%/decade and the probability to belong to the permanent sea-ice seasonal cycle has decreased by 1.5%/decade. In the first order, the area between the Central Arctic and the open-ocean does not belong to a unique cluster but to a mix of the four clusters. Little trend is seen for the likelihood of belonging to the partial winter-freezing cluster and the full winter-freezing cluster but spatial shifts are seen. We also introduce another diagnostic which labels the regime changes of the Arctic sea-ice. The zone from the northern Chukchi to the Laptev Seas has already lost their typical seasonal cycle (destabilization) with the loss of permanent sea-ice and the Barents-Kara Seas and Chukchi Sea have now a new typical seasonal cycle (stabilization) associated with the extension of the open-ocean cluster.

The k-means clustering of the sea-ice seasonal cycle we applied to the Arctic shares similarities with the analysis of Wachter et al. (2021) for the Antarctic. The main differences however reside in our use of Mahalanobis distances, to account for the correlation between the months, and the initialization based on equal separation of quantiles for the centroids, to avoid any random aspect in the clustering algorithm. These two choices enable to constrain the clustering with physical features.

https://doi.org/10.5194/egusphere-2025-704
Preprint. Discussion started: 6 March 2025

Our clustering approach is complementary to diagnostics involving the dates of melting and freezing onsets, which have been used to quantify changes in the duration and shift of ice-free seasons at the pan or regional Arctic scales (Markus et al., 2009; Stammerjohn et al., 2012; Parkinson 2014; Johnson & Eicken, 2016; Stroeve et al., 2014; Lebrun et al., 2019). Instead, our method enables us to target regions experiencing a shift to a typical seasonal cycle representing longer and shifted ice-free seasons, and retrieve the year of the shift. Another advantage is that we do not use any arbitrary cutoff of sea-ice concentration. Additionally, our diagnostic delimits regions with the same sea-ice seasonal dynamics. The major limit of our approach resides in the exact grid point quantification of the real seasonal cycle features, as we gather grid cells within a type represented by a single seasonal cycle (the centroid). Considering the full seasonal cycle gives useful information, as its derivative gives the period of melting and growth. Therefore, the two diagnostics complement each other nicely.

By doing the diagnostic of the trend in the length of the sea-ice season for the period 1979-2013, Parkinson (2014) shows that the length of the ice season has shortened in almost all the coastal regions (around -10 days/decade with a maximum -30 days/decade in the northern Chukchi Sea and around -50 days/decade in the northern Barents Sea), the main exceptions being the Bering Sea, portions of the Canadian Archipelago (around +10 days/decade) and the central Arctic where the sea-ice season duration remain unchanged over the period. Similar features are obtained in Lebrun et al., (2019) who considered the period up to 2015. This is consistent with our results showing a decrease in probability for the permanent sea-ice cluster almost everywhere (especially in the Pacific side but not in the Bering Sea and the Canadian Archipelago), leading to a shortening of the seasonal cycle. The year of loss in the likelihood to belong to the permanent sea-ice shows a smooth displacement northward, being therefore in a destabilization state. Also, the seasonal cycle from the Barents Sea to the Baffin Bay shifted from 1979-1990s toward the open-ocean cluster. Moreover, we were able to demonstrate that in the 1979-1990s, the Chukchi Sea and northern Hudson Bay, and around the 2000s' the Kara Seas stabilized toward the partial winter-freezing cluster.

https://doi.org/10.5194/egusphere-2025-704
Preprint. Discussion started: 6 March 2025

The clustering optimally splits the seasonal cycles having a summer opening into two types: partial winter-freezing (a sinusoidal shape with a long ice-free period) and full winter-freezing cluster (an abrupt shape with a short ice-free period). Our clustering results suggest that, considering a given location fully ice-covered in a given winter, the next summer will be ice-free if the sea ice starts to melt in April, and will not be ice-free if the melting starts in May. And, considering a given ice-free location in summer, the next winter will be fully ice-covered if the freezing starts in October which is not the case if the freezing starts in November. Therefore, it appears that the starting date of melting and freezing could be key for predicting ice conditions around 6 months in advance. This feature follows a physical behaviour of sea-ice shown by Stammerjohn (2012) and Stroeve et al. (2016). They found strong correlations between the dates of the spring sea-ice retreat and subsequent autumn sea-ice advance (i.e., over the summer), indicating that an early sea-ice retreat is often followed by a late autumn sea-ice advance and conversely, a late sea-ice retreat is often followed by an early autumn sea-ice advance. Indeed, consistent with our clustering analysis, the partial winter-freezing cluster has an early sea-ice retreat (in March) and late autumn sea-ice advance (mid-October) while the full winter-freezing cluster has a late sea-ice retreat (in April) and early autumn sea-ice advance (mid-September).

Concerning the growth and melting of sea-ice, Parkinson et al., 1999 and Parkinson and Cavalieri, 2008 showed that the seasonal decay of sea ice extent is gradual during early summer and then accelerates during the remaining summer months, whereas wintertime growth is most rapid in early winter. A standard explanation suggests that this asymmetry between seasonal growth and decay is caused by rapid temperature changes driven by air masses from the Eurasian continent [Peixoto and Oort, 1992]. Here this asymmetry in the seasonal cycle is seen only for the permanent sea-ice cluster and full winter freezing cluster, suggesting that the partial winter sea-ice is driven by another driver.

In the first order, these partial and full winter freezing clusters are located in the same region (a belt between the Central Arctic and the open-ocean). In the second order (i.e with a probability difference of around 10% for the whole period),

https://doi.org/10.5194/egusphere-2025-704
Preprint. Discussion started: 6 March 2025

the full winter-freezing cluster (with no sinusoidal feature) is more likely present along the Arctic coastline than the partial winter-freezing cluster (with a sinusoidal feature). The reason for this spatial repartition could be explained by the fact that the sinusoidal feature of the sea-ice seasonal cycle is linked to the ability of the ice to freeze and expand freely, without being blocked by land, as suggested by Eisenman (2010).

The introduction in this paper of the clustering of the Arctic sea-ice seasonal cycle, with its statistical aspect, can provide an approach to validate the dynamics of sea-ice in climate models. Indeed, applying the clustering method described here to models could inform if a given model has the same number of optimal clusters and the types of seasonal cycles as the one obtained from observations. It could also be used to answer how different clusters will be distributed for different future scenarios. Overall, this methodology is transposable to other variables to better answer its past and future variability in a robust statistical framework.

Author's contribution

All authors contributed to the conceptual design of the study and the interpretation of the results. PT, FS and AS established the methodological framework. AS developed the code, generated the figures, and drafted the initial version of the article. PT, FS, and CL carefully revised the paper contributing to its improvement.

Financial support

This study is funded by ANR and France 2030 through the project CLIMArcTIC (grant ANR-22-POCE-0005)

References

Aksenov, Y., Popova, E. E., Yool, A., Nurser, A. G., Williams, T. D., Bertino, L., & Bergh, J. (2017). On the future navigability of Arctic sea routes: High-resolution projections of the Arctic Ocean and sea ice. *Marine Policy*, *75*, 300-317.

Bushuk, M., Ali, S., Bailey, D. A., Bao, Q., Batté, L., Bhatt, U. S., ... & Zhang, Y. (2024). Predicting September Arctic Sea Ice: A Multi-Model Seasonal Skill Comparison. *Bulletin of the American Meteorological Society*.

Cavalieri, D. J., Gloersen, P., & Campbell, W. J. (1984). Determination of sea ice parameters with the Nimbus 7 SMMR. Journal of Geophysical Research: Atmospheres, 89(D4), 5355-5369.

Cocetta, F., Zampieri, L., Selivanova, J., & Iovino, D. (2024). Assessing the representation of Arctic sea ice and the marginal ice zone in ocean–sea ice reanalyses. *The Cryosphere*, *18*(10), 4687-4702.

Cohen, J., Zhang, X., Francis, J., Jung, T., Kwok, R., Overland, J., Ballinger, T. J., Bhatt, U. S., Chen, H. W., Coumou, D., Feldstein, S., Gu, H., Handorf, D., Henderson, G., Ionita, M., Kretschmer, M., Laliberte, F., Lee, S., Linderholm, H. W., and Yoon, J.: Divergent consensus on Arctic amplification influence on mid-latitude severe winter weather, Nat. Clim. Change, 10, 20–29, https://doi.org/10.1038/s41558-019-0662-y, 2020

Comiso, J. C. (1986). Characteristics of Arctic winter sea ice from satellite multispectral microwave observations. Journal of Geophysical Research: Oceans, 91(C1), 975-994.

Delhaye, S., Massonnet, F., Fichefet, T., Msadek, R., Terray, L., & Screen, J. (2024). Dominant role of early winter Barents–Kara sea ice extent anomalies in subsequent atmospheric circulation changes in CMIP6 models. Climate Dynamics, 62(4), 2755-2778.

Deser, C., Tomas, R. A., and Sun, L.: The role of ocean–atmosphere coupling in the zonal-mean atmospheric response to Arctic sea-ice loss, J. Climate, 28, 2168–2186, 2015.

Forster, P., T. Storelvmo, K. Armour, W. Collins, J.-L. Dufresne, D. Frame, D.J. Lunt, T. Mauritsen, M.D. Palmer, M. Watanabe, M. Wild, and H. Zhang, 2021: The Earth's Energy Budget, Climate Feedbacks, and Climate Sensitivity. In Climate Change 2021: The Physical Science Basis. Contribution of Working Group I to the Sixth Assessment Report of the Intergovernmental Panel on Climate Change [Masson-Delmotte, V., P. Zhai, A. Pirani, S.L. Connors, C. Péan, S. Berger, N. Caud, Y. Chen, L. Goldfarb, M.I. Gomis, M. Huang, K. Leitzell, E. Lonnoy, J.B.R. Matthews, T.K. Maycock, T. Waterfield, O. Yelekçi, R. Yu, and B. Zhou (eds.)]. Cambridge University Press, Cambridge, United Kingdom and New York, NY, USA, pp. 923–1054, doi:10.1017/9781009157896.009.

Fox-Kemper, B., H.T. Hewitt, C. Xiao, G. Aðalgeirsdóttir, S.S. Drijfhout, T.L. Edwards, N.R. Golledge, M. Hemer, R.E. Kopp, G. Krinner, A. Mix, D. Notz, S. Nowicki, I.S. Nurhati, L. Ruiz, J.-B. Sallée, A.B.A. Slangen, and Y. Yu, 2021: Ocean,Cryosphere and

https://doi.org/10.5194/egusphere-2025-704
Preprint. Discussion started: 6 March 2025

Sea Level Change. In Climate Change 2021: The Physical Science Basis. Contribution of Working Group I to the Sixth Assessment Report of the Intergovernmental Panel on Climate Change [Masson-Delmotte, V., P. Zhai, A. Pirani, S.L. Connors, C. Péan, S. Berger, N. Caud, Y. Chen, L. Goldfarb, M.I. Gomis, M. Huang, K. Leitzell, E. Lonnoy, J.B.R. Matthews, T.K. Maycock, T. Waterfield, O. Yelekçi, R. Yu, and B. Zhou (eds.)]. Cambridge University Press, Cambridge, United Kingdom and New York, NY, USA, pp. 1211–1362, doi:10.1017/9781009157896.011.

Galley, R. J., Else, B. G. T., Prinsenberg, S. J., Babb, D., & Barber, D. G. (2013). Summer sea ice concentration, motion, and thickness near areas of proposed offshore oil and gas development in the Canadian Beaufort Sea—2009. *Arctic*, 105-116.

GEBCO Compilation Group. (2024). GEBCO 2024 Grid. doi:10.5285/1c44ce99-0a0d-5f4f-e063-7086abc0ea0f . Date Accessed: 6 Feb. 2025

Goosse, H., Kay, J. E., Armour, K. C., Bodas-Salcedo, A., Chepfer, H., Docquier, D., ... & Vancoppenolle, M. (2018). Quantifying climate feedbacks in polar regions. *Nature communications*, *9*(1), 1919.

Gulev, S.K., P.W. Thorne, J. Ahn, F.J. Dentener, C.M. Domingues, S. Gerland, D. Gong, D.S. Kaufman, H.C. Nnamchi, J. Quaas, J.A. Rivera, S. Sathyendranath, S.L. Smith, B. Trewin, K. von Schuckmann, and R.S. Vose, 2021: Changing State of the Climate System. In Climate Change 2021: The Physical Science Basis. Contribution of Working Group I to the Sixth Assessment Report of the Intergovernmental Panel on Climate Change [Masson-Delmotte, V., P. Zhai, A. Pirani, S.L. Connors, C. Péan, S. Berger, N. Caud, Y. Chen, L. Goldfarb, M.I. Gomis, M. Huang, K. Leitzell, E. Lonnoy, J.B.R. Matthews, T.K. Maycock, T. Waterfield, O. Yelekçi, R. Yu, and B. Zhou (eds.)]. Cambridge University Press, Cambridge, United Kingdom and New York, NY, USA, pp. 287–422, doi:10.1017/9781009157896.004.

Huntington, H. P., Quakenbush, L. T. & Nelson, M. Evaluating the effects of climate change on indigenous marine mammal hunting in northern and western alaska using traditional knowledge. Front. Mar. Sci. 4, 319 (2017)

Houghton, I. A., & Wilson, J. D. (2020). El Niño detection via unsupervised clustering of Argo temperature profiles. Journal ofGeophysical Research: Oceans, 125, e2019JC015947. https://doi.org/10.1029/2019JC015947

Huntington, H. P., Danielson, S. L., Wiese, F. K., Baker, M., Boveng, P., Citta, J. J., ... & Wilson, C. (2020). Evidence suggests potential transformation of the Pacific Arctic ecosystem is underway. Nature Climate Change, 10(4), 342-348.

IPCC, 2019: Summary for Policymakers. In: IPCC Special Report on the Ocean and Cryosphere in a Changing Climate [H.-O. Pörtner, D.C. Roberts, V. Masson-Delmotte, P. Zhai, M. Tignor, E. Poloczanska, K. Mintenbeck, A. Alegría,M. Nicolai, A. Okem, J. Petzold, B. Rama, N.M. Weyer (eds.)]. Cambridge University Press, Cambridge, UK andNew York, NY, USA, pp. 3–35. https://doi.org/10.1017/9781009157964.001.

https://doi.org/10.5194/egusphere-2025-704
Preprint. Discussion started: 6 March 2025

IPCC, 2021: Summary for Policymakers. In: Climate Change 2021: The Physical Science Basis. Contribution of Working Group I to the Sixth Assessment Report of the Intergovernmental Panel on Climate Change [Masson-Delmotte, V., P. Zhai, A. Pirani, S.L. Connors, C. Péan, S. Berger, N. Caud, Y. Chen, L. Goldfarb, M.I. Gomis, M. Huang, K. Leitzell, E. Lonnoy, J.B.R. Matthews, T.K. Maycock, T. Waterfield, O. Yelekçi, R. Yu, and B. Zhou (eds.)]. Cambridge University Press, Cambridge, United Kingdom and New York, NY, USA, pp. 3–32, doi:10.1017/9781009157896.001.

Jain, A. K. (2010). Data clustering: 50 years beyond K-means. *Pattern recognition letters*, *31*(8), 651-666.

Johannessen, O. M., Kuzmina, S. I., Bobylev, L. P., & Miles, M. W. (2016). Surface air temperature variability and trends in the Arctic: new amplification assessment and regionalisation. Tellus A: Dynamic Meteorology and Oceanography, 68(1), 28234.

Johnson, M., & Eicken, H. (2016). Estimating Arctic sea-ice freeze-up and break-up from the satellite record: A comparison of different approaches in the Chukchi and Beaufort Seas. Elementa, 4, 000124.

Kwok, R. (2007). Near zero replenishment of the Arctic multiyear sea ice cover at the end of 2005 summer. Geophysical Research Letters, 34(5).

Lee, J.-Y., J. Marotzke, G. Bala, L. Cao, S. Corti, J.P. Dunne, F. Engelbrecht, E. Fischer, J.C. Fyfe, C. Jones, A. Maycock, J. Mutemi, O. Ndiaye, S. Panickal, and T. Zhou, 2021: Future Global Climate: Scenario-Based Projections and Near-Term Information. In Climate Change 2021: The Physical Science Basis. Contribution of Working Group I to the Sixth Assessment Report of the Intergovernmental Panel on Climate Change [Masson-Delmotte, V., P. Zhai, A.Pirani, S.L. Connors, C. Péan, S. Berger, N. Caud, Y. Chen, L. Goldfarb, M.I. Gomis, M. Huang, K. Leitzell, E. Lonnoy, J.B.R. Matthews, T.K. Maycock, T. Waterfield, O. Yelekçi, R. Yu, and B. Zhou (eds.)]. Cambridge University Press, Cambridge, United Kingdom and New York, NY, USA, pp. 553–672, doi:10.1017/9781009157896.006.

Levine, X. J., Cvijanovic, I., Ortega, P., Donat, M. G., & Tourigny, E. (2021). Atmospheric feedback explains disparate climate response to regional Arctic sea-ice loss. npj Climate and Atmospheric Science, 4(1), 28.
Meier, W. N., Stroeve, J., & Fetterer, F. (2007). Whither Arctic sea ice? A clear signal of decline regionally, seasonally and extending beyond the satellite record. Annals of Glaciology, 46, 428-434.

Mao, J., & Jain, A. K. (1996). A self-organizing network for hyperellipsoidal clustering (HEC). *Ieee transactions on neural networks*, *7*(1), 16-29.

Maslanik, J., J. Stroeve, C. Fowler, and W. Emery (2011), Distribution and trends in Arctic sea ice age through spring 2011, Geophys. Res. Lett., 38, L13502, doi:10.1029/2011GL047735.

Meier, W. N., F. Fetterer, A. K. Windnagel, and J. S. Stewart. (2021). NOAA/NSIDC Climate Data Record of Passive Microwave Sea Ice Concentration, Version 4 [Data Set]. Boulder, Colorado USA. National Snow and Ice Data Center. https://doi.org/10.7265/efmz-2t65. Date Accessed 15-07-2024.

Meier, W. N., Stewart, J. S., Windnagel, A., & Fetterer, F. M. (2022). Comparison of hemispheric and regional sea ice extent and area trends from NOAA and NASA passive microwave-derived climate records. *Remote Sensing*, *14*(3), 619.

Meier, W. N., & Stroeve, J. (2022). An updated assessment of the changing Arctic sea ice cover. *Oceanography*, *35*(3/4), 10-19.

Meier, Walter N., and J. Scott Stewart. (2023). NSIDC Land, Ocean, Coast, Ice, and Sea Ice Region Masks. NSIDC Special Report 25. Boulder CO, USA: National Snow and Ice Data Center. https://nsidc.org/sites/default/files/documents/technical-reference/nsidc-special-report-25.pdf

Parkinson, C. L. (2014), Spatially mapped reductions in the length of the Arctic sea ice season, Geophys. Res. Lett., 41, 4316–4322, doi:10.1002/2014GL060434

Parkinson, C. L., and J. C. Comiso (2013), On the 2012 record low Arctic sea ice cover:
Combined impact of preconditioning and an August storm,Geophys. Res. Lett., 40, 1356–1361, doi:10.1002/grl.50349

Parkinson, C.L.; Comiso, J.C.; Zwally, H.J.; Cavalieri, D.J.; Gloersen, P.; Campbell, W.J. Arctic Sea Ice, 1973–1976: Satellite Passive-Microwave Observations; NASA SP-489; National Aeronautics and Space Administration: Washington, DC, USA, 1987; p. 296.
Peng, G., & Meier, W. N. (2018). Temporal and regional variability of Arctic sea-ice coverage from satellite data. Annals of Glaciology, 59(76pt2), 191-200.

Pedregosa, F., Michel, V., Grisel, O., Blondel, M., Prettenhofer, P., Weiss, R., et al. (2011). Scikit-learn: Machine learning in Python

Pithan, F., & Mauritsen, T. (2014). Arctic amplification dominated by temperature feedbacks in contemporary climate models. *Nature geoscience*, *7*(3), 181-184.

Petty, A. A., Stroeve, J. C., Holland, P. R., Boisvert, L. N., Bliss, A. C., Kimura, N., & Meier, W. N. (2018). The Arctic sea ice cover of 2016: a year of record-low highs and higher-than-expected lows. *The Cryosphere*, *12*(2), 433-452.

Przybylak, R. 2002. Variability of air temperature and atmospheric precipitation in the Arctic. Dordrecht, etc., Kluwer Academic Publishers

https://doi.org/10.5194/egusphere-2025-704
Preprint. Discussion started: 6 March 2025

Przybylak, R. (2007). Recent air-temperature changes in the Arctic. *Annals of Glaciology*, *46*, 316-324.

Regan, H. C., Rampal, P., Ólason, E., Boutin, G., & Korosov, A. (2022). Modelling the evolution of Arctic multiyear sea ice over 2000–2018. *The Cryosphere Discussions*, *2022*, 1-28.

Ricker, R., Hendricks, S., Kaleschke, L., Tian-Kunze, X., King, J., and Haas, C.: A weekly Arctic sea-ice thickness data record from merged CryoSat-2 and SMOS satellite data, The Cryosphere, 11, 1607–1623, https://doi.org/10.5194/tc-11-1607-2017, 2017.

Rousseeuw, P. J. (1987). Silhouettes: a graphical aid to the interpretation and validation of cluster analysis. *Journal of computational and applied mathematics*, *20*, 53-65.

Shu, Q., Wang, Q., Årthun, M., Wang, S., Song, Z., Zhang, M., & Qiao, F. (2022). Arctic Ocean Amplification in a warming climate in CMIP6 models. Science advances, 8(30), eabn9755.

Siddon, E. C., Zador, S. G., & Hunt Jr, G. L. (2020). Ecological responses to climate perturbations and minimal sea ice in the northern Bering Sea. Deep Sea Research Part II: Topical Studies in Oceanography, 181, 104914.

Simon, A., Gastineau, G., Frankignoul, C., Rousset, C., and Codron, F.: Transient climate response to Arctic sea-ice loss with two ice-constraining methods, J. Climate, 34, 3295–3310, https://doi.org/10.1175/JCLI-D-20-0288.1, 2021.

Smith, L. C., & Stephenson, S. R. (2013). New Trans-Arctic shipping routes navigable by midcentury. Proceedings of the National Academy of Sciences, 110(13), E1191-E1195.

Smith, D. M., Eade, R., Andrews, M. B., Ayres, H., Clark, A., Chripko, S., and Walsh, A.: Robust but weak winter atmospheric circulation response to future Arctic sea-ice loss, Nat. Commun., 13, 1–15, 2022

Stammerjohn, S., Massom, R., Rind, D., and Martinson, D.: Regions of rapid sea ice change: An inter-hemispheric seasonal comparison, Geophys. Res. Lett., 39, L06501, https://doi.org/10.1029/2012GL050874, 2012.

Stock, C. A. et al. Reconciling fisheries catch and ocean productivity. Proc. Natl Acad. Sci. USA 114, E1441–E1449 (2017).

Stroeve, J. C., T. Markus, L. Boisvert, J. Miller, and A. Barrett (2014), Changes in Arctic melt season and implications for sea ice loss, Geophys. Res. Lett., 41, 1216–1225, doi:10.1002/2013GL058951.

Stroeve, J. C., Crawford, A. D., and Stammerjohn, S.: Using timing of ice retreat to predict timing of fall freeze-up in the Arctic, Geophys. Res. Lett., 43, GL069314,

https://doi.org/10.5194/egusphere-2025-704
Preprint. Discussion started: 6 March 2025

https://doi.org/10.1002/2016GL069314, 2016.

Sutherland, P., & Dumont, D. (2018). Marginal ice zone thickness and extent due to wave radiation stress. *Journal of Physical Oceanography*, *48*(8), 1885-1901.

Valko, I. (2014). Differentiating Arctic provinces: a cluster analysis of geographic and geopolitical indicators. Central European Journal of International & Security Studies, 8(4).

Vancoppenolle, M., L. Bopp, G. Madec, J. Dunne, T. Ilyina, P. R. Halloran, and N. Steiner (2013), Future Arctic Ocean primary productivity from CMIP5 simulations: Uncertain outcome, but consistent mechanisms, Global Biogeochem. Cycles, 27, 605–619, doi:10.1002/gbc.20055.

Wachter, P., Reiser, F., Friedl, P., & Jacobeit, J. (2021). A new approach to classification of 40 years of Antarctic sea ice concentration data. International Journal of Climatology, 41, E2683-E2699.